

Comparison of the Accuracy of Different CFD Turbulence Models for the Prediction of the Climatic Parameters in a Tunnel Greenhouse

R. Nebbali
LMSE, Université
Mouloud Mammeri
de Tizi-Ouzou,
15000 Tizi-Ouzou,
Algérie

J.C. Roy
FEMTO-ST,
CREST, Université
de Franche-Comté,
2, Avenue Jean
Moulin, 90000
Belfort, France

T. Boulard
INRA –URIH,
400, route des
Chappes, BP 167,
06903 Sophia-
Antipolis, France

S. Makhoulouf
LMSE, Université
Mouloud Mammeri
de Tizi-Ouzou,
15000 Tizi-Ouzou,
Algérie

Keywords : greenhouse, tunnel, ventilation, CFD, velocity, temperature, humidity, sonic anemometer.

Abstract

This paper presents a comparative study of numerical simulations and experimental determination of dynamic and climatic parameters in a greenhouse. The objective of this work is the determination of the accuracy of different turbulence models ($k-\varepsilon$ Standard, $k-\varepsilon$ RNG and $k-\varepsilon$ Realizable) included in the Fluent[®] CFD package and used to predict velocity and climatic fields in large scale domains and for low characteristic velocity.

For that purpose simulations have been carried out for an empty tunnel-type greenhouse with lateral vents, located in Avignon, southern France. The equations of flow are solved with the Fluent[®] CFD package inside and outside the greenhouse. Several series of experimental measurements have been previously carried out using sonic anemometers (Boulard *et al.*, 2000) and a comparative study between measured and calculated values at 48 nodal points of the greenhouse is presented. It is shown that for the three turbulence models, errors on obtained results for temperature as well as humidity remain relatively weak. However, accuracy on velocity modulus as well as on turbulent kinetic energy is more significant in high circulation areas than in other low ones.

Neglecting the fluctuations induced by the instability of the measured boundary conditions (intensity and direction of the wind) and the intrusive nature of the measurement tools (sonic anemometers) the experimental data allow us to easily compare the three models. For this tunnel greenhouse arrangement, the $k-\varepsilon$ Standard turbulence model comes out to be the more accurate among the three considered ones.

INTRODUCTION

The complexity of the equations describing the phenomena intervening in a greenhouse has oriented many researchers towards experimental approaches. Indeed, many experimental studies allowed quantifying the mass and heat transfers intervening in greenhouses with crops. Fuchs (1990), Boulard & Baille (1993) established a relation between the evapotranspiration and the characteristics of the greenhouse cover and control equipments (screens, fog, heating and ventilation systems). Ventilation rate calculations use the tracer gas method (Bot, 1983; de Jong, 1990; Boulard and Baille, 1995; Kittas *et al.*, 1995) which is very expensive and difficult to realize for large scale

greenhouses. Another semi-empirical approach, based on the greenhouse energy balance (Demrati *et al.*, 2001), offers a good approximation for high ventilation rates, but with a larger uncertainty for low wind speed values (Boulard and *al.*, 1993; Wang and Boulard, 2000 ; Fernandez and Bailey, 1992).

Recent development of computational fluid dynamics tools turns numerous researchers to the use of numerical techniques. The turbulent regime which prevails in the greenhouses has to be considered. However, as the DNS (direct numerical simulation) approach imply a prohibiting computing time, other simplified approaches based on the statistical decomposition of the turbulent flow into an average and a fluctuating component (Reynolds decomposition) must be considered. Moreover, supposing the isotropy of the Reynold's tensor led us to distinguish different turbulence models such as the Standard k- ϵ , k- ϵ Realizable and k- ϵ RNG (renormalization group model).

This paper presents a comparative study of numerical simulations with a previous experimental determination of dynamic and climatic parameters in a tunnel greenhouse located in Avignon (Boulard *et al.*, 2000), with in view a determination of the accuracy of the different turbulence models which are already included in the Fluent[®] CFD package. More particularly, this study aims to predict velocity and climatic fields in a large inside scale domains, for low characteristic velocity.

MATERIALS AND METHODS

Greenhouse tunnel description

Scalar (air temperature, relative humidity and turbulence components) and vectorial (air speed) fields have been experimentally mapped in an empty greenhouse tunnel type of $22 \times 8 \text{ m}^2$ ground surface. Ventilation was performed by vent openings which were realized by a simple spacing of the plastic sheets on both sides of the greenhouse using pieces of wood (Fig. 1).

The velocity modulus, the air temperature and humidity and the turbulence components were measured in two cross sections of the tunnel, one section (I) in the middle between two successive openings and the other (II), at the level of the openings (Fig. 1). The velocity modulus, the air temperature and the turbulence components were obtained by means of two 3-dimensional sonic anemometers, (omni directional, R3, research ultrasonic anemometer, Gill R&D) and air humidity deduced from two Krypton hygrometers measurements (Campbell, Utah). During the experiment, the ground was continuously humidified to simulate a humid surface similar to a crop cover.

With only two sampling positions possible at any time, a difficulty arise from how to deal with changing external conditions throughout the time to measure the 24 different measurement positions within each cross section (Fig; 2). This was overcome by selecting measurements for a fixed prevailing North wind condition and by using external reference wind speed and difference in air temperature and humidity as scaling parameters (see Boulard *et al.*, 2000).

The CFD code

The CFD code Fluent v. 6.1 has been used to perform the simulations of the flow patterns presented in this study. This code solves the 3D conservation equations for physical quantities transported in the flow like mass, momentum, energy and water vapour concentration. The governing equations of flow are discretized in the domain of interest and are transformed into a linear equations system using the finite volumes

method. The linear equations system, together with the boundary conditions, is then solved with the SIMPLE algorithm: pressure and velocity components are first determined with a prediction-correction method followed by the determination of the temperature and water vapour concentration fields.

The domain model

The domain of calculation is made up of a large parallelepiped (82m × 68m × 24m) which includes the empty greenhouse tunnel type (22m × 8m × 3m) (Fig.3). The dimensions of this domain were chosen large enough to insure the independence of airflow to the boundaries locations.

The meshing of the domain was determined with two characteristic sizes: 0.15 m meshes inside the tunnel and 1 m meshes outside. Consequently, two structured meshes have been defined and connected together with an unstructured mesh (Fig.4). The grid is more refined near the floor (0.10 m) and near the walls and the vents (0.05 m) of the tunnel where strong velocity gradients are supposed to be found. The choice of this grid was validated after several trials in order to both optimise the computational time and the precision of the model, especially in the vents. A logarithmic wind profile deduced from experimental measurements (Haxaire, 1999) has been used to model the atmospheric wind at the inlet boundary of the domain (located from North). A reference velocity of 3.8m s⁻¹ has been defined at a 5m reference. Hence, inlet velocity u has been defined as:

$$u = \frac{u_*}{K} \ln\left(\frac{z}{z_0}\right)$$

with u_* the friction velocity ($u_*=0.28ms^{-1}$); K the Von Karman constant ($K=0.41$) and z_0 the friction length ($z_0=0.0193m$). Inlet temperature ($T_0=14.4^\circ C$), inlet relative humidity ($RH_0=53\%$), plastic cover temperature ($T_{S7}=16.5^\circ C$, $T_{S8}=13.7^\circ C$, $T_{S10}=14.4^\circ C$, $T_{S5}=16.4^\circ C$, $T_{S3}=17.5^\circ C$, $T_{S4}=19.4^\circ C$, $T_{S13}=20.2^\circ C$, $T_{S11}=21.8^\circ C$), ground temperature ($T_{S9}=18.5^\circ C$, $T_{S1}=17.0^\circ C$, $T_{S14}=19.3^\circ C$, $T_{S6}=22.2^\circ C$, $T_{S2}=24.1^\circ C$) (Fig. 2) and ground relative humidity ($RH_S=100\%$) were also determined from experimental data. The turbulent kinetic energy and the turbulent dissipation rate are described by the following expressions (Hoxey and Richardson (1993)) :

$$k = \frac{u_*^2}{\sqrt{C_\mu}} \quad \text{and} \quad \varepsilon = \frac{u_*^3}{K(z + z_0)}$$

The turbulence models

The classic turbulence model is based on the Reynolds decomposition, which consists to superpose the field of average values of the flow variables with the fluctuations of these values. This gives place to the Reynolds tensor. The calculation of this tensor, for the assumption of isotropy, uses two additional equations for the turbulent kinetic energy k and for the turbulent dissipation rate ε . This approach constitutes the core of the two-equation turbulence models (k - ε models). The Fluent CFD code permits the use of three of such models: the Standard, RNG and Realizable k - ε models. These semi-empirical models have been validated for different flow patterns such around a cylinder, on a plate plane and for a jet through an opening.

When compared to the Standard k - ε model, RNG model derives from a rigorous statistical technique, called Renormalization Groups Theory. It presents a similar form when compared to the standard model. However, it includes the following modifications:

-An additive term in the equation for ε , which improves accuracy in the calculation of the turbulent stresses.

-The taking into account of more swirl effects on turbulence, what represents a good simulation of swirl flows.

-A formula for the calculation of the turbulent Prandtl number, while the standard model uses a constant value.

-Whereas the standard model offers good performances in high Reynolds number areas, RNG model proposes an analytical relation for the calculation of turbulent viscosity, which takes into account the low Reynolds number areas.

Realizable model has the same structure as the standard and RNG $k-\varepsilon$ models, except for the model constants.

RESULTS AND DISCUSSION

Comparison of numerical and experimental data

In order to evaluate the most representative model of flow, heat and mass transfers prevailing in the greenhouse, a comparative study between measured values and calculated data has been carried out for climatic and dynamic variables: temperature, humidity, velocity modulus and turbulent kinetic energy. Most of the measurements points are located in the vicinity of the walls, where strong gradients of the measured variables are occurred.

Figures (5) to (12) present the evolution of these various variables on the lines 1 of sections I and II. Figures (13) to (16) present the distribution of the error on each section for each variable (noted Φ_r) and for each measurement location (noted j). The error Φ_r is defined as:

$$\Phi_r(j) = \frac{\Phi_c(j) - \Phi_{mes}(j)}{\Phi_{mes}(j)}$$

Were:

$$\overline{\Phi_{mes}} = \frac{\sum_{j=1(\text{section I})}^{24} \Phi_{mes}(j) + \sum_{j=1(\text{section II})}^{24} \Phi_{mes}(j)}{48} \text{ and } \Phi = \{|V|, T, RH, k\}$$

An average value of these errors is calculated for the two sections, using the relations:

$$\Phi_I = \frac{\sum_{j=1(\text{section I})}^{24} \Phi_r(j)}{24} \text{ and } \Phi_{II} = \frac{\sum_{j=1(\text{section II})}^{24} \Phi_r(j)}{24}$$

Figures (17) and (18) present these distributions. This makes it possible to evaluate the order of magnitude of the difference between measured and calculated values. From these results it appears that the three models of turbulence represent in a similar way the evolution of the velocity modulus along a horizontal line (line 1) that joins the measurements locations n° 6, 9, 13, 17 and 24 in the section II. The variation becomes more important for the low velocity field located in section I (Fig.5). Indeed, for section II, the error of the velocity modulus would remain weak for the different model of turbulence by disregarding positions 2, 3 and 6, (Fig. 14). Concerning both temperature and humidity, the three models successfully compute the distribution of these variables on the whole domain (Fig. 9 to 12). They give an error lower than 10% for the

temperature field (Fig. 17) whereas the Standard $k-\epsilon$ model shows the lowest value of the error on humidity for both sections (Fig. 18).

CONCLUSION

A comparison between three models of turbulence in the Fluent CFD code has been carried out in order to determine the velocity field and the climatic parameters distribution in an empty greenhouse tunnel. Numerical results have been compared with experimental values. Concerning the dynamic variables, on the level of section II, characterized by high velocity, the error remains weak, whereas for the low speeds located at the level of section I, the error becomes important. Indeed, on the locations characterized by low velocity, the air flow is much more affected by the sonic anemometer, which constitutes an intrusive measurement technique of the velocity field. This in turn affects the measurements of the turbulent kinetic energy. Thus, the important variations between measured and calculated values which relate to these two types of dynamic can be partially allotted to measurement errors. The choice of the model of turbulence will thus be determined by the comparative study carried out on the field of temperature and humidity. For these variables of agronomic interest, the three models simulate in a satisfactory way their distribution in the greenhouse. However, the Standard $k-\epsilon$ model gives the lowest error value and it can be chosen as it represents a good compromise between the complexity of calculation and the realism in the simulation of turbulence.

Literature cited

- Boulard, T., Wang, S., Haxaire, R.; 2000; Mean and turbulent air flows and microclimatic patterns in an empty greenhouse tunnel. *Agricultural and forest Meteorology* 100 , 169-181).
- Boulard, T., Baille, A., 1995. Modelling of air exchange rate in a greenhouse equipped with continuous roof vents. *Journal of Agricultural Engineering Research*, 61, 37-48.
- Boulard, T. and Baille, A., 1993. A simple greenhouse climate control model incorporating effects of aeration and evaporative cooling. *Agricultural and Forest Meteor.*, 65, 145-157.
- Boulard, T., Baille, A., Draoui, B., 1993. Greenhouse natural ventilation measurements and modelling. *International workshop AGRITECH on cooling Systems in Greenhouses* (Fuchs, M., Segal, I., Teitel, M., eds), Tel Aviv, Israel, pp 24-34.
- Bot, G.P.A, 1983. Greenhouse climate: from physical process to a dynamic model. PhD thesis, Agricultural University Wageningen, The Netherlands.
- de Jong, T., 1990. Natural ventilation of large multi-span greenhouses. PhD Thesis, Agricultural University Wageningen, The Netherlands.
- Fuchs, M., 1990. Effect of transpiration on greenhouse cooling. *Proceedings of the international seminar on British-Israel workshop on greenhouse technology.* Agricultural Research Organisation, Bet Dagan Israel, 155-181.
- Haxaire, R. 1999. Caractérisation et modélisation des écoulements d'air dans une serre. Thèse de Doctorat, Université de Nice, Sophia-Antipolis.
- Hoxey, R. P and Richardson G. M, 1983; Measurements of wind loads on full scale plastic greenhouse. *J. of Wind Engineering and Industrial Aerodynamics*, 16: 57-83.
- Kittas, C., Draoui, B., Boulard, T., 1995. Quantification du taux d'aération d'une serre à ouvrant continu en toiture. [Quantification of the ventilation of greenhouse with a roof opening.] *Agricultural and Forest Meteorology*, 77, 95-111.

Wang, S., Boulard, T., 2000. Predicting the microclimate in a naturally ventilated plastichouse in a Mediterranean climate. *Journal of Agricultural Engineering Research*, 75, 27-38.

Notation

C_μ : constant for the turbulence model. ε : dissipation rate of the turbulent kinetic energy. k : turbulent kinetic energy. K : Von Karman constant. Φ_c : calculated variable Φ_{mes} : measured variable RH_0 : inlet air humidity.	RH_s : ground surface humidity. T_o : inlet air temperature. T_s : ground surface or cover temperature. u_* : friction velocity. $ V $: velocity modulus. z_o : friction length.
--	--

Figures

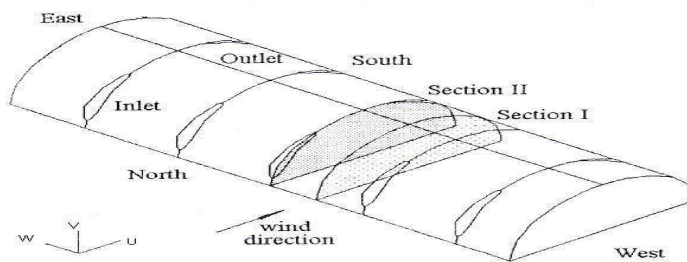


Fig.1: Schematic view of the experimental plastic tunnel. The symbols u, v, w correspond to the three components of the air velocity measured by sonic anemometry (Boulard *et al.*, 2000) in two sections (I and II).

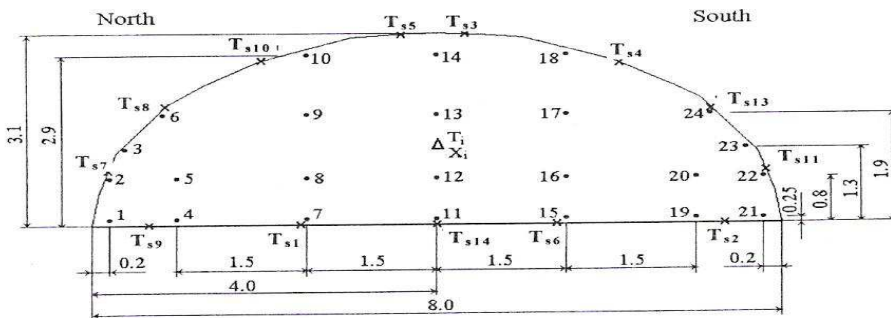


Fig.2: Measurement locations (1 to 24) in the central section of the tunnel. All dimensions are in metres. $\{Ts_j - Ts_{j4}\}$: surface temperature measurements; Δ : reference location

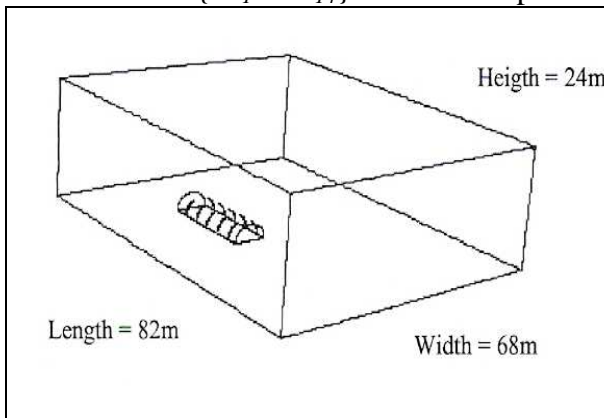


Fig 3: Sketch of the large domain model

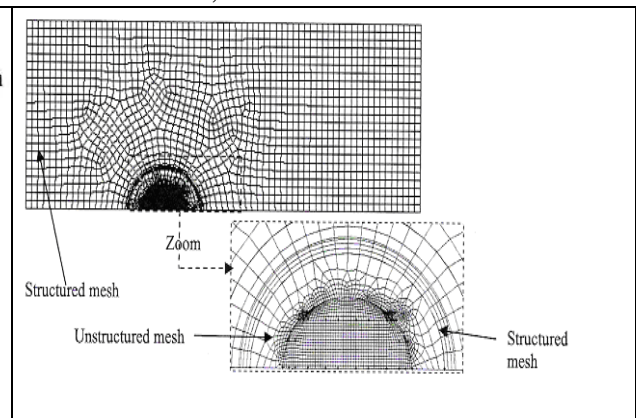


Fig 4: Sketch of the mesh of the tunnel

Section I

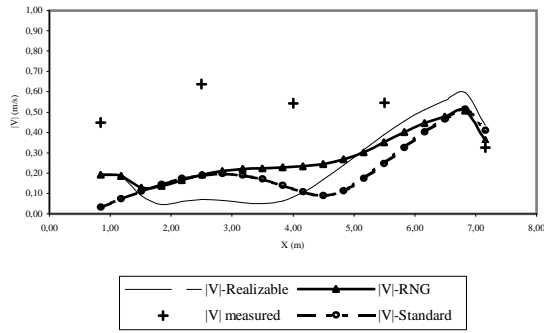


Fig 5: Velocity modulus along line 1

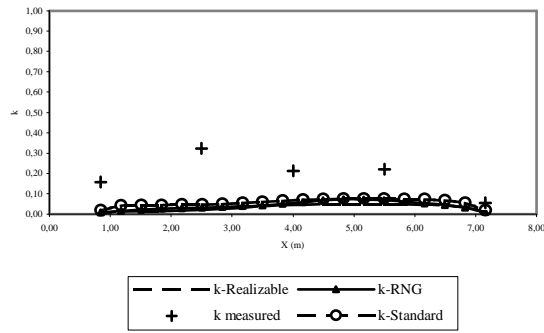


Fig 7: Turbulent kinetic energy along line 1

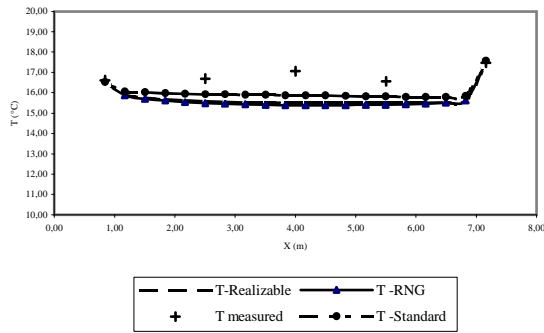


Fig 9: Temperature along line 1

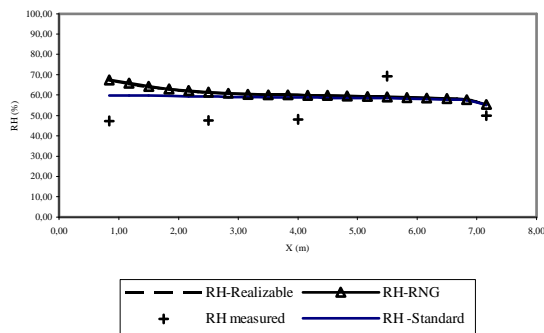


Fig 11: Relative humidity along line 1

Section II

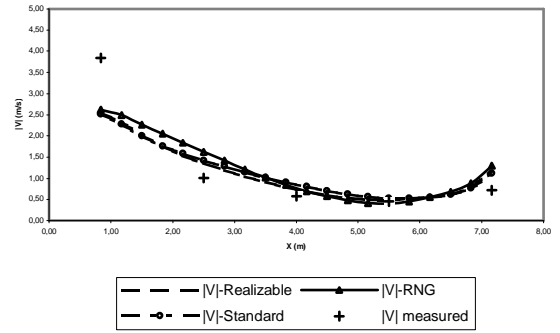


Fig 6: Velocity modulus along line 1

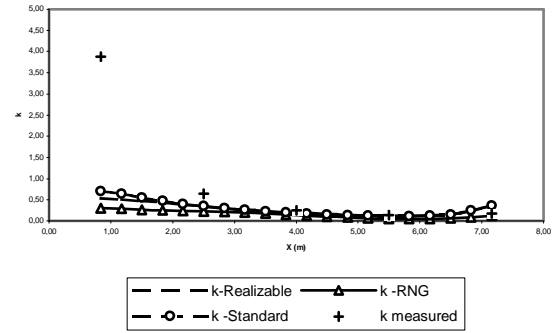


Fig 8: Turbulent kinetic energy along line 1

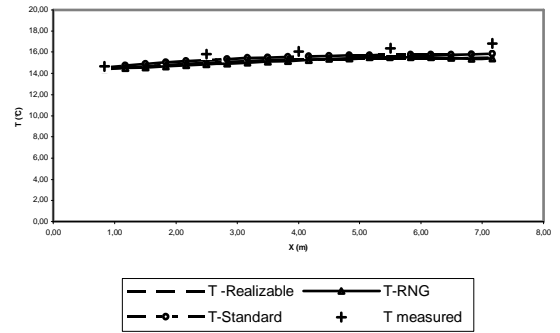


Fig 10: Temperature along line 1

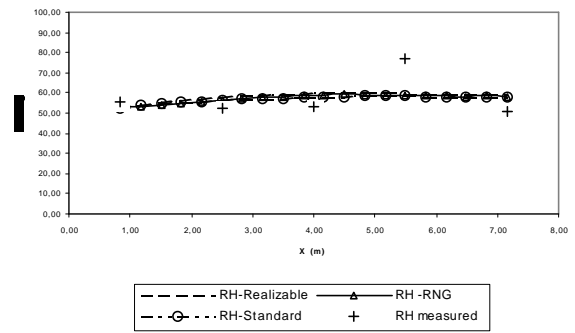


Fig 12: Relative humidity along line 1

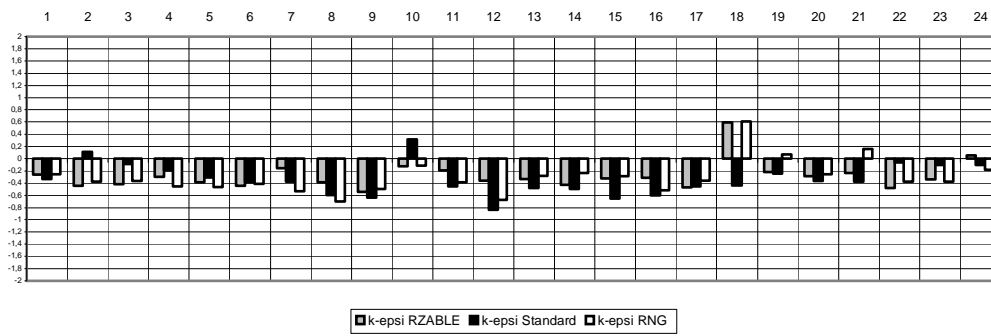


Fig 13: Error distribution of the velocity modulus in section I

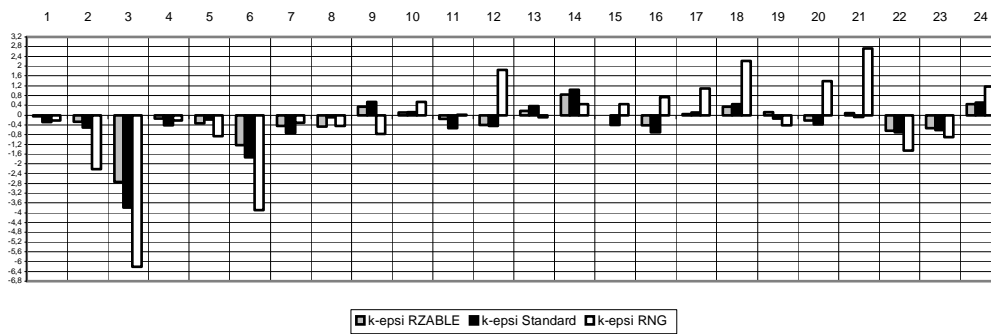


Fig 14: Error distribution of the velocity modulus in section II

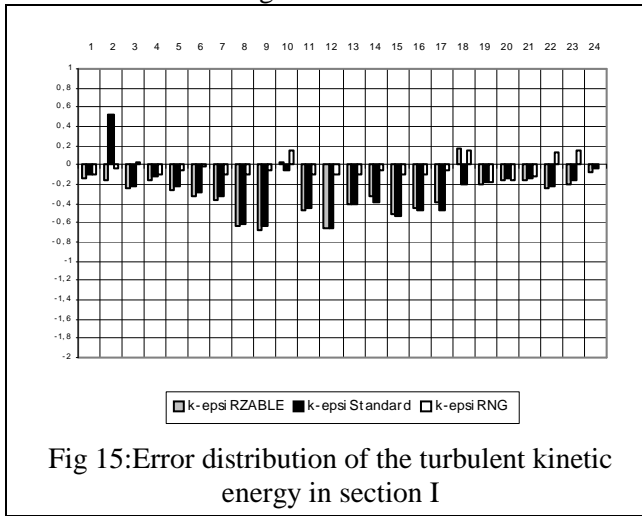


Fig 15: Error distribution of the turbulent kinetic energy in section I

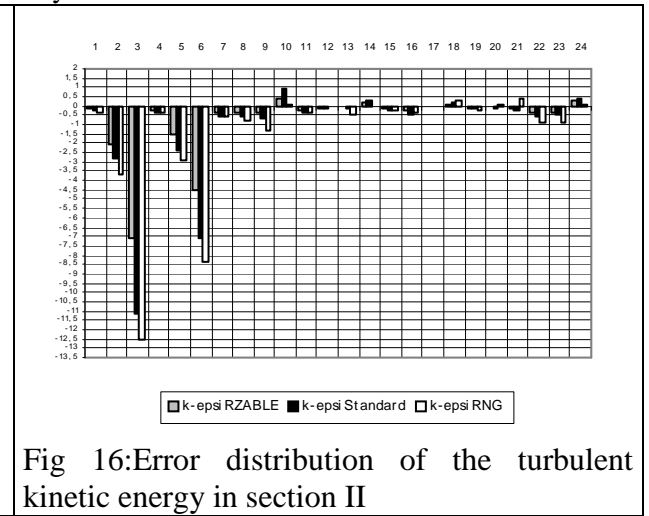


Fig 16: Error distribution of the turbulent kinetic energy in section II

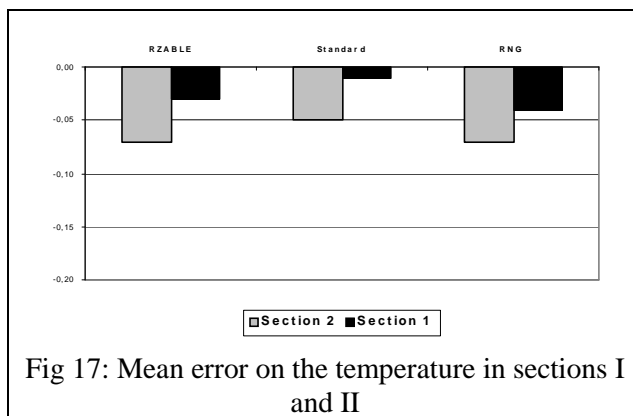


Fig 17: Mean error on the temperature in sections I and II

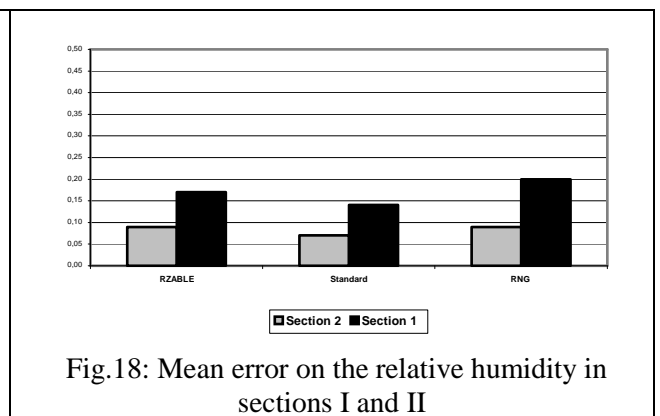


Fig 18: Mean error on the relative humidity in sections I and II